

# Energy & Environmental Science

Accepted Manuscript



This is an *Accepted Manuscript*, which has been through the Royal Society of Chemistry peer review process and has been accepted for publication.

*Accepted Manuscripts* are published online shortly after acceptance, before technical editing, formatting and proof reading. Using this free service, authors can make their results available to the community, in citable form, before we publish the edited article. We will replace this *Accepted Manuscript* with the edited and formatted *Advance Article* as soon as it is available.

You can find more information about *Accepted Manuscripts* in the [Information for Authors](#).

Please note that technical editing may introduce minor changes to the text and/or graphics, which may alter content. The journal's standard [Terms & Conditions](#) and the [Ethical guidelines](#) still apply. In no event shall the Royal Society of Chemistry be held responsible for any errors or omissions in this *Accepted Manuscript* or any consequences arising from the use of any information it contains.

Cite this: DOI: 10.1039/c0xx00000x

www.rsc.org/xxxxxx

ARTICLE TYPE

# Solution-processed bulk heterojunction solar cells based on a porphyrin small molecule with 7% power conversion efficiency

Hongmei Qin,<sup>†</sup> Lisheng Li,<sup>†</sup> Fangqing Guo, Shijian Su, Junbiao Peng, Yong Cao, Xiaobin Peng\*

Received (in XXX, XXX) Xth XXXXXXXXXX 20XX, Accepted Xth XXXXXXXXXX 20XX

DOI: 10.1039/b000000x

A porphyrin small molecule with less bulky substituents at porphyrin periphery has been synthesized as the donor material, which exhibits a power conversion efficiency up to 7.23% under AM 1.5G irradiation (100 mW cm<sup>-2</sup>) for the solution processed bulk heterojunction solar cells with PC<sub>61</sub>BM as the acceptor material.

Solution-processed bulk heterojunction (BHJ) organic solar cells (OSCs) are drawing more and more attention because of their potential for the mass production of flexible, lightweight and cost-effective devices, therefore have been the focus of considerably academic and industrial research.<sup>1-5</sup> During recent years, significant improvements have been achieved in BHJ solar cells through the combination of the molecular design of active materials and interface layers, morphology control, and fabricating techniques,<sup>4, 6-10</sup> and power conversion efficiencies (PCEs) over 9% have been achieved.<sup>11, 12</sup>

Solution processable small molecules (SMs) for BHJ OSCs are very attractive for several advantages such as defined molecular structure and molecular weight, high purity, and less batch-to-batch variations superior to their polymer counterparts,<sup>13</sup> showing a promising future in low-cost and large-scale OSC commercialization applications.<sup>14-17</sup> And the performance of solution processed SM BHJ solar cells has been steadily increased over the past few years, which is closing the gap of the best polymer solar cells (PSCs).<sup>18-22</sup> For example, Bazan and Heeger et al. first reported a PCE of 6.7% for the BHJ OSCs based on a small molecule with 3,3'-di-2-ethylhexylsilylene as the core unit.<sup>23</sup> And the PCE was further enhanced to 7.0% and to 9.02% after the optimizations of chemical structures and devices with a conventional architecture.<sup>24, 25</sup> On the other hand, Chen et al. synthesized a serial of small molecules with a benzo[1,2-b:4,5-b']dithiophene (BDT) unit as the central building block and the best PCE was first reported to be 5.44%.<sup>26</sup> After a serial of molecular structure optimizations, the PCE was then enhanced to 7.38%, and finally to 8.12%.<sup>27-29</sup>

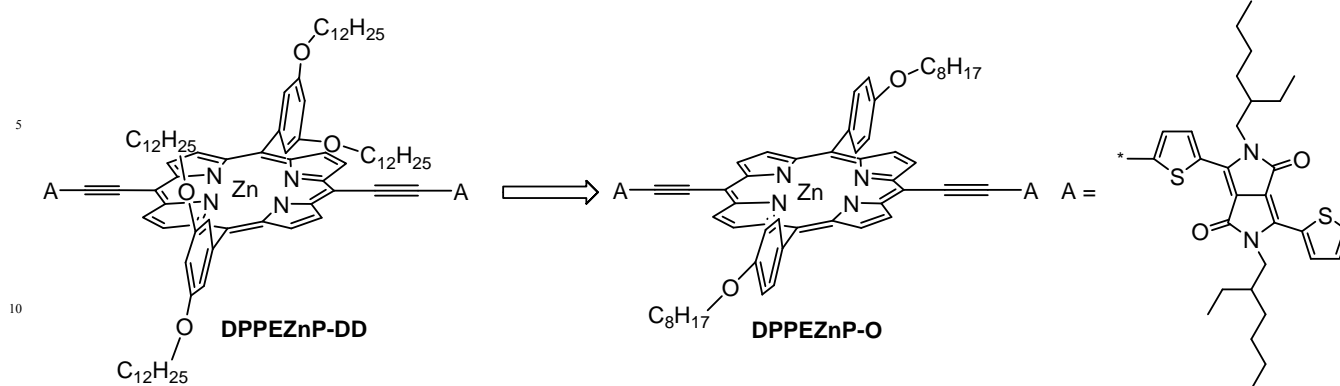
However, SM BHJ solar cells have not been investigated as intensively as PSCs, and their overall performance still remains below that of their polymer counterparts. To date, only the above mentioned two category SM donor materials were reported with

PCEs over 7% when blended with fullerene derivatives in solution processed BHJ solar cells. Therefore, many lessons from BHJ PSCs should be applied on the design of OSC materials and device engineering to further improve the PCEs of SM-based BHJ OSCs. Currently, the active materials, especially the donor materials, are still the most important for high PCE OSCs. Therefore, much more efforts should be made on the design and the understanding of the structure–property–function relationships of the active materials.

Inspired by the natural photosynthetic systems, which utilize chlorophylls to absorb light and carry out photochemical charge separation to store light energy, porphyrins and their derivatives have been explored as the active materials from the beginning of OSC studies, but the PCEs of the solution processed BHJ OSCs based on them were usually very low.<sup>30-34</sup> In order to facilitate the intramolecular charge transport, we introduced ethynylene to link a porphyrin core with different acceptor units to make the porphyrin core conjugated to the acceptor units recently, and high PCEs of 4–5% were achieved for the solution processed BHJ OSCs by employing them as donor materials with [6,6]-phenyl C<sub>61</sub>-butyric acid methyl ester (PC<sub>61</sub>BM) and [6,6]-phenyl C<sub>71</sub>-butyric acid methyl ester (PC<sub>71</sub>BM) as the acceptors.<sup>35, 36</sup>

Though high performance was obtained, better PCEs could be expected on more delicate molecular design of the porphyrins. For example, we previously employed two bulky 3,5-di(dodecyloxy)-phenyl substituents to warranty the solubility of the porphyrins. But the long chains of dodecyloxy groups at 3,5-positions of a phenyl ring stick out of the porphyrin plane and can in turn suppress the intermolecular  $\pi$ - $\pi$  stacking, and therefore may lead to a relatively poorer photovoltaic performance.<sup>37</sup> In this study, 4-octyloxy-phenyl groups are used in place of 3,5-di(dodecyloxy)-phenyl ones and a new conjugated donor-acceptor porphyrin – 5,15-bis(2,5-bis-(2-ethyl-hexyl)-3,6-dithienyl-2-yl-2,5-dihydro-pyrrolo[3,4-c]pyrrole-1,4-dione-5'-yl-ethynyl)-10,20-bis(4-octyloxy-phenyl)-porphyrin zinc (DPPEZnP-O, Scheme 1) is designed and synthesized, which also shows excellent solubility in organic solvents such as chloroform and toluene.

85



Scheme 1. The chemical structure of DPPEZnP-O.

DPPEZnP-O was synthesized by Sonogashira coupling reaction as the reported procedures shown in Supplementary Information.<sup>36</sup> As shown in Figure 1, DPPEZnP-O exhibits broad and strong optical absorption coverage in visible and near infrared (NIR) region both in solution and thin film. In dichloromethane, the absorption peaks are observed at 459, 565 and 736 nm. Cast as a thin film, DPPEZnP-O exhibits absorption peaks at 462, 572, a very weak shoulder peak at 736 and a strong peak at 813 nm. The significant red-shift of nearly 80 nm from 736 nm in solution to 813 nm in film is attributed to the strong intermolecular  $\pi$ - $\pi$  stacking in the condensed solid state,<sup>38</sup> which could be beneficial to a higher hole mobility and photovoltaic performance for OSCs.<sup>39</sup> Compared with the weak shoulder peak at 790 nm of DPPEZnP-DD,<sup>36</sup> the peak of DPPEZnP-O at 813 nm is red-shifted and its intensity is increased significantly, indicating that DPPEZnP-O exhibits stronger cofacial  $\pi$ - $\pi$  stacking than that of DPPEZnP-DD in film. These optical behaviours confirm that the modification with the less bulky substituents at the porphyrin periphery of DPPEZnP-O effectively promotes its intermolecular  $\pi$ - $\pi$  interactions in solid state.

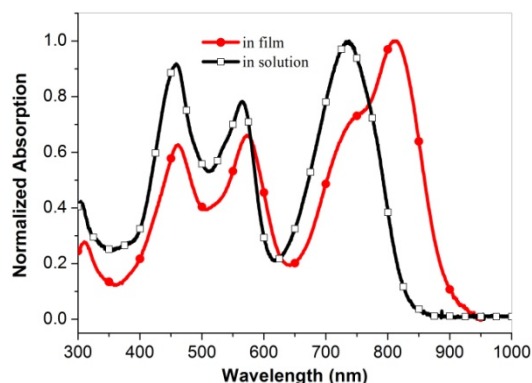


Figure 1. UV-Vis-NIR absorption spectra of DPPEZnP-O in  $\text{CH}_2\text{Cl}_2$  solution and in film.

levels of DPPEZnP-O, we investigated the redox behaviours of DPPEZnP-O by electrochemical cyclic voltammetry (CV) in acetonitrile containing 0.1 M  $\text{Bu}_4\text{NPF}_6$  as the supporting electrolyte and a saturated calomel electrode as the reference electrode. The onset oxidation ( $E_{\text{ox}}$ ) and reduction ( $E_{\text{red}}$ ) potentials of DPPEZnP-O are 0.67 and -0.80 V vs. saturated calomel electrode, respectively, from which the highest occupied molecular orbital (HOMO) and the lowest unoccupied molecular orbital (LUMO) energy levels are estimated to be -5.07 and -3.60 eV according to the empirical formula of  $E_{\text{HOMO}} = -e(E_{\text{ox}} + 4.40)$  (eV) and  $E_{\text{LUMO}} = -e(E_{\text{red}} + 4.40)$  (eV), respectively. The band gap is 1.47 eV, which is similar with the optical band gap of 1.36 eV obtained from the onset of the absorption spectrum in film.

BHJ OSCs were fabricated by solution processing with a general device structure of indium tin oxide (ITO)/ poly(styrene sulfonate)-doped poly(ethylene-dioxythiophene) (PEDOT:PSS)/ DPPEZnP-O:PC<sub>61</sub>BM/ poly[(9,9-bis(3'-(N,N-dimethylamino)propyl)-2,7-fluorene)-alt-2,7-(9,9-dioctylfluorene) (PFN)]/Al and were measured under AM 1.5 illumination, 100  $\text{mW cm}^{-2}$ .<sup>40</sup> As shown in Figure 2 and listed in Table 1, when processed without any additive, the best device provides a PCE up to 5.83% with an open circuit voltage ( $V_{\text{OC}}$ ), a short circuit current ( $J_{\text{SC}}$ ) and a fill factor ( $FF$ ) of 0.74 V, 14.97  $\text{mA cm}^{-2}$ , and 52.64%, respectively. And the average PCE reaches to 5.62%, which is enhanced by 57% compared with that of the OSC devices based on DPPEZnP-DD.<sup>36</sup>

Table 1. Photovoltaic properties of the OSCs based on DPPEZnP-O/PC<sub>61</sub>BM (1:1.2, w/w) under the illumination of AM1.5 G, 100  $\text{mW cm}^{-2}$ .

Solvent	$J_{\text{SC}}$ ( $\text{mA cm}^{-2}$ )	$V_{\text{OC}}$ (V)	$FF$ (%)	PCE (%)
W/O	14.97	0.74	52.64	5.83 <sup>a</sup> (5.62±0.15) <sup>b</sup>
0.4% DIO	16.00	0.71	63.67	7.23 <sup>a</sup> (6.83±0.21) <sup>b</sup>

<sup>a</sup>) The best PCE. <sup>b</sup>) The average value of PCE±standard deviation of ten devices.

In order to obtain the information of the frontier orbital energy

Different from the case of DPPEZnP-DD, pyridine did not play a positive role to the performance of the OSCs based on DPPEZnP-

O.<sup>41</sup> However, when the widely-used additive 1,8-diiodo-octane (DIO) was employed,<sup>42</sup> the performance of the OSCs based on DPPEZnP-O was enhanced significantly. The typical  $J$ - $V$  characteristics and photovoltaic parameters of the OSCs containing 0.4% DIO as a processing additive during the spin-casting are also shown in Figure 2 and listed in Table 1, respectively. The best device, which was processed with 0.4% DIO, provides us with a PCE up to 7.23% (with  $V_{OC} = 0.71$  V,  $J_{SC} = 16.0$  mA cm<sup>-2</sup>, and  $FF = 63.67\%$ ), and the average PCE of ten devices is 6.83%. In comparison with those of the best devices based on DPPEZnP-DD, the photovoltaic parameters changed significantly are  $J_{SC}$  and  $FF$ , which are increased from 11.88 to 16.00 mA cm<sup>-2</sup> and from 50.2% to 63.67%, respectively, while the  $V_{OC}$  only slightly decreased from 0.80V to 0.71V. Since the molecular structures of DPPEZnP-O and DPPEZnP-DD are quite similar, the significant enhancement of  $J_{SC}$  and  $FF$  is mainly ascribed to the stronger intermolecular  $\pi$ - $\pi$  stacking of DPPEZnP-O in film. To the best of our knowledge, this PCE is the highest for the solution processed BHJ OSCs based on porphyrin derivatives,<sup>43</sup> and DPPEZnP-O also ranks to one of the best small molecule donor materials with the above mentioned two category small molecules that showed PCEs over 7% for solution processed BHJ OSCs.

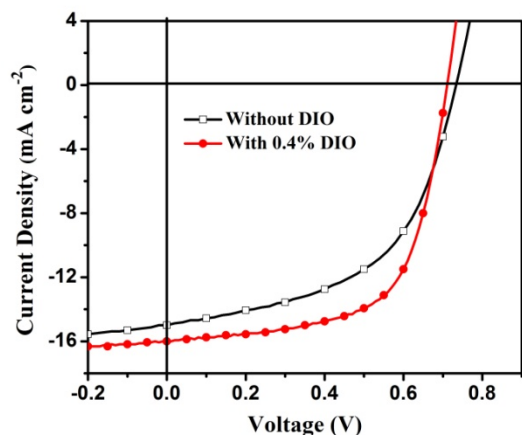


**Figure 2.**  $J$ - $V$  characteristics of the OSCs based on DPPEZnP-O/PC<sub>61</sub>BM blends (1:1.2, w/w) processed with 0.4% DIO additive.

We measured the external quantum efficiencies (EQEs) of the devices processed with and without DIO. As shown in Figure 3, all these devices processed with and without DIO additive show a very wide range of photocurrent generation in the region from 380 to 900 nm, and the EQEs in the whole region increased when DIO was used. For example, the EQE values at 570 nm and 805 nm increases from 47% to 57% and from 52% to 58%, respectively, after the addition of 0.4% DIO.

The morphologies of the blend films processed with and without DIO were investigated by atomic force microscopy (AFM) to gain insight into the performance enhancement upon the replacement of the substituents and the introduction of DIO additive.<sup>44</sup> As shown in Figure 4, the AFM height phase images show no apparently crystalline domains for all the films with and without DIO. And the root-mean-square (RMS) roughness values of the pristine film and the film processed with DIO are 0.857

nm (Figure 4a) and 0.345 nm (Figure 4b), respectively, which are much smaller than those of the blend films of DPPEZnP-DD/PC<sub>61</sub>BM.<sup>36</sup> The lower RMS roughness of these blend films indicate that DPPEZnP-O shows better miscibility with PC<sub>61</sub>BM, and may form a finer interpenetrating network to facilitate both exciton separation and charge transport. The phase topography of the pristine film (Figure 4c) exhibits microscale phase separation, which is also better than that of DPPEZnP-DD/PC<sub>61</sub>BM film.<sup>36</sup> Furthermore, the film of DPPEZnP-O/PC<sub>61</sub>BM processed with DIO shows even much smaller phase separation domains (Figure 4d), which are very suitable for efficient exciton dissociation and charge transporting and should lead to an increased  $J_{SC}$  and  $FF$  for a corresponding solar cell.<sup>45, 46</sup>

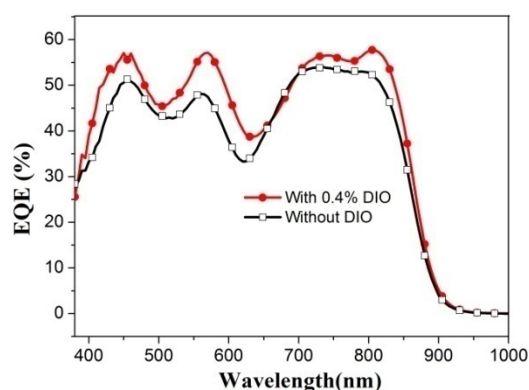


**Figure 3.** The EQE curves of the devices based on DPPEZnP-O/PC<sub>61</sub>BM blends (1:1.2, w/w) processed without and with 0.4% DIO.

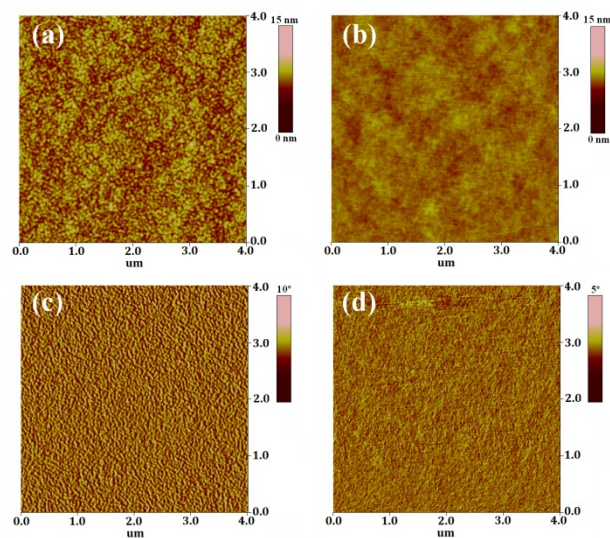


**Figure 4.** Tapping mode AFM height (a, b) and phase images (c, d) (4×4 μm) of thin films of DPPEZnP-O:PC<sub>61</sub>BM (1:1.2, w/w) with (b, d) and without 0.4% DIO (a, c).

To have a better understanding of the morphologies, we recorded transmission electron microscopy (TEM) images of the blend films processed without and with 0.4% DIO (Figure S1). Consistent with the AFM results, TEM images also show that the

blend films possess rather uniform and fine features, which can be ascribed to the good miscibility of DPPEZnP-O with PC<sub>61</sub>BM. With the addition of 0.4% DIO, the film forms even more continuous interpenetrating networks, which ensure more D/A interfaces and thus lead to enhanced  $J_{SC}$  and  $FF$ .

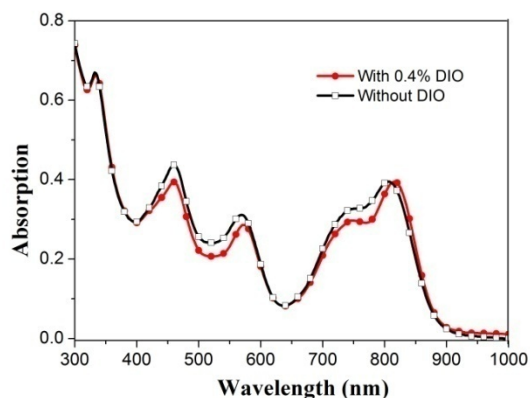


**Figure 5.** UV-Vis-NIR absorption spectra of the DPPEZnP-O/PC<sub>61</sub>BM (1:1.2, w/w) blend films prepared without and with DIO additive.

UV-Vis-NIR absorption spectra of the blend films with PC<sub>61</sub>BM processed with and without DIO additive were also measured to extract more information from the BHJ layers. These films were spin-cast under the identical conditions as the fabrication of the OSC devices and the absorption spectra were not normalized. As shown in Figure 5, the NIR peak is red-shifted from 806 nm to 815 nm after addition of DIO, which is characteristic for films that yield higher-efficiency solar cells.<sup>39</sup>

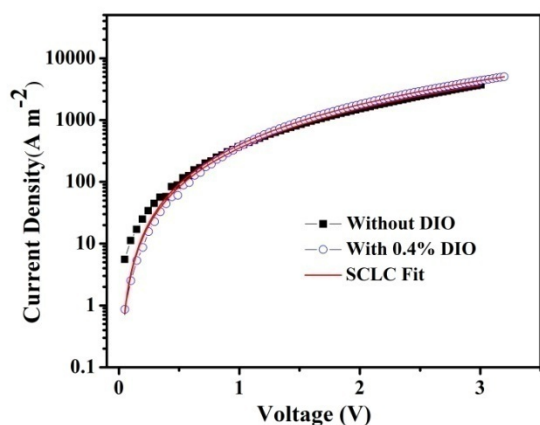


**Figure 6.**  $J$ - $V$  characteristics of the hole-only devices processed with and without DIO in configuration of ITO/PEDOT:PSS/active layer/MoO<sub>3</sub>/Al.

We fabricated hole-only devices with almost the same thickness as the solar cells by spin-casting DPPEZnP-O/PC<sub>61</sub>BM with and without DIO using MoO<sub>3</sub> as the buffer layer at the cathode to block the injection of electrons and measured the hole mobilities directly,<sup>47</sup> which were obtained through space charge limited current (SCLC) method,<sup>48</sup> and the  $J$ - $V$  curves for the hole-only devices are shown in Figure 6. The hole mobility of the device fabricated without DIO is  $2.38 \times 10^{-4} \text{ cm}^2 \text{V}^{-1} \text{S}^{-1}$ , and enhanced to

$4.68 \times 10^{-4} \text{ cm}^2 \text{V}^{-1} \text{S}^{-1}$  for the device in the presence of 0.4% DIO additive. Both values are larger than the best value of  $1.6 \times 10^{-4} \text{ cm}^2 \text{V}^{-1} \text{S}^{-1}$  based on DPPEZnP-DD.<sup>36</sup> Apparently, the replacement of 3,5-di(dodecyloxy)-phenyl groups by 4-octyloxy-phenyl ones in DPPEZnP-O and the addition of DIO additive both improve the hole transmission performance of the devices, and the enhancement is ascribed to the better intermolecular  $\pi$ - $\pi$  stacking of DPPEZnP-O and more suitable surface morphology for OSCs in film.

## Conclusion

In summary, a narrow band gap porphyrin small molecule with the less bulky substituents at porphyrin periphery was designed and synthesized to simultaneously facilitate the intramolecular charge transport and increase the intermolecular  $\pi$ - $\pi$  stacking in film. The solution processed BHJ OSCs based on this porphyrin provided us with a power conversion efficiency up to 7.23%, which is the highest PCE of solution-processed BHJ solar cells based on porphyrins and their derivatives to date and also ranks to one of the best small molecule donor materials with other two category small molecules that showed PCEs over 7% for solution processed BHJ OSCs. Since the properties of porphyrins can be easily tuned via synthetic modifications at the periphery, we speculate that there is still great room for designing more favourable porphyrin small molecules for higher performance solar cells. Our results also demonstrate that the performance of BHJ OSCs based on small molecules can be significantly enhanced through careful molecular designs and device optimizations.

## Acknowledgements

This work was financially supported by the grants from the National Natural Science Foundation of China (51073060, 50990065, and 51010003), International Science & Technology Cooperation Program of China (2010DFA52150 and 2013DFG52740), and the Guangdong Natural Science Foundation (No. S2012030006232).

## Notes and references

*Institute of Polymer Optoelectronic Materials and Devices, State Key Laboratory of Luminescent Materials and Devices, South China University of Technology, 381 Wushan Road, Guangzhou 510640, China Fax: (+)86-20-87110606; Tel:86-20-87114346, E-mail: chxbpeng@scut.edu.cn*

† These authors contributed equally to this work.

70

† Electronic Supplementary Information (ESI) available: [details of any supplementary information available should be included here]. See DOI: 10.1039/b000000x/

1. G. Yu, J. Gao, J. C. Hummelen, F. Wudl and A. J. Heeger, *Science*, 1995, **270**, 1789-1791.
2. G. Li, V. Shrotriya, J. S. Huang, Y. Yao, T. Moriarty, K. Emery and Y. Yang, *Nat. Mater.*, 2005, **4**, 864-868.

3. S. H. Park, A. Roy, S. Beaupre, S. Cho, N. Coates, J. S. Moon, D. Moses, M. Leclerc, K. Lee and A. J. Heeger, *Nat. Photon.*, 2009, **3**, 297-U295.
4. Y. Liang, Z. Xu, J. Xia, S.-T. Tsai, Y. Wu, G. Li, C. Ray and L. Yu, *Adv. Mater.*, 2010, **22**, E135-E138.
5. S. B. Darling and F. You, *Rsc Adv.*, 2013, **3**, 17633-17648.
6. S. Guenes, H. Neugebauer and N. S. Sariciftci, *Chem. Rev.*, 2007, **107**, 1324-1338.
7. B. C. Thompson and J. M. J. Frechet, *Angew. Chem. Int. Ed.*, 2008, **47**, 58-77.
8. X. Yang and J. Loos, *Macromolecules*, 2007, **40**, 1353-1362.
9. B. Kippelen and J.-L. Bredas, *Energy Environ. Sci.*, 2009, **2**, 251-261.
10. Y.-J. Cheng, S.-H. Yang and C.-S. Hsu, *Chem. Rev.*, 2009, **109**, 5868-5923.
11. Z. He, C. Zhong, S. Su, M. Xu, H. Wu and Y. Cao, *Nat. Photon.*, 2012, **6**, 591-595.
12. Y. Li, *Acc. Chem. Res.*, 2012, **45**, 723-733.
13. M. P. Nikiforov, B. Lai, W. Chen, S. Chen, R. D. Schaller, J. Strzalka, J. Maser and S. B. Darling, *Energy Environ. Sci.*, 2013, **6**, 1513-1520.
14. Y. Li, Q. Guo, Z. Li, J. Pei and W. Tian, *Energy Environ. Sci.*, 2010, **3**, 1427-1436.
15. B. Walker, C. Kim and T.-Q. Nguyen, *Chem. Mater.*, 2011, **23**, 470-482.
16. A. Mishra and P. Baeuerle, *Angew. Chem. Int. Ed.*, 2012, **51**, 2020-2067.
17. S.-W. Chiu, L.-Y. Lin, H.-W. Lin, Y.-H. Chen, Z.-Y. Huang, Y.-T. Lin, F. Lin, Y.-H. Liu and K.-T. Wong, *Chem. Commun.*, 2012, **48**, 1857-1859.
18. S. Shen, P. Jiang, C. He, J. Zhang, P. Shen, Y. Zhang, Y. Yi, Z. Zhang, Z. Li and Y. Li, *Chem. Mater.*, 2013, **25**, 2274-2281.
19. Z. E. Ooi, T. L. Tam, R. Y. C. Shin, Z. K. Chen, T. Kietzke, A. Sellinger, M. Baumgarten, K. Mullen and J. C. deMello, *J. Mater. Chem.*, 2008, **18**, 4619-4622.
20. J. E. Anthony, *Chem. Mater.*, 2011, **23**, 583-590.
21. Y. Lin, Y. Li and X. Zhan, *Chem. Soc. Rev.*, 2012, **41**, 4245-4272.
22. Y. Liu, Y. M. Yang, C.-C. Chen, Q. Chen, L. Dou, Z. Hong, G. Li and Y. Yang, *Adv. Mater.*, 2013, **25**, 4657-4662.
23. Y. M. Sun, G. C. Welch, W. L. Leong, C. J. Takacs, G. C. Bazan and A. J. Heeger, *Nat. Mater.*, 2012, **11**, 44-48.
24. T. S. van der Poll, J. A. Love, N. Thuc-Quyen and G. C. Bazan, *Adv. Mater.*, 2012, **24**, 3646-3649.
25. V. Gupta, A. K. K. Kyaw, D. H. Wang, S. Chand, G. C. Bazan and A. J. Heeger, *Sci. Rep.*, 2013, **3**.
26. Y. Liu, X. Wan, F. Wang, J. Zhou, G. Long, J. Tian and Y. Chen, *Adv. Mater.*, 2011, **23**, 5387-5391.
27. Z. Li, G. He, X. Wan, Y. Liu, J. Zhou, G. Long, Y. Zuo, M. Zhang and Y. Chen, *Adv. Energy Mater.*, 2012, **2**, 74-77.
28. J. Zhou, Y. Zuo, X. Wan, G. Long, Q. Zhang, W. Ni, Y. Liu, Z. Li, G. He, C. Li, B. Kan, M. Li and Y. Chen, *J. Am. Chem. Soc.*, 2013, **135**, 8484-8487.
29. J. Zhou, X. Wan, Y. Liu, Y. Zuo, Z. Li, G. He, G. Long, W. Ni, C. Li, X. Su and Y. Chen, *J. Am. Chem. Soc.*, 2012, **134**, 16345-16351.
30. C. W. Tang, *Appl. Phys. Lett.*, 1986, **48**, 183-185.
31. A. Kay and M. Gratzel, *J. Phys. Chem.*, 1993, **97**, 6272-6277.
32. M. Victoria Martinez-Diaz, G. de la Torre and T. Torres, *Chem. Commun.*, 2010, **46**, 7090-7108.
33. M. G. Walter, A. B. Rudine and C. C. Wamser, *J. Porphyrins Phthalocyanines*, 2010, **14**, 759-792.
34. T. Hasobe, H. Imahori, P. V. Kamat, T. K. Ahn, S. K. Kim, D. Kim, A. Fujimoto, T. Hirakawa and S. Fukuzumi, *J. Am. Chem. Soc.*, 2005, **127**, 1216-1228.
35. Y. Huang, L. Li, X. Peng, J. Peng and Y. Cao, *J. Mater. Chem.*, 2012, **22**, 21841-21844.
36. L. Li, Y. Huang, J. Peng, Y. Cao and X. Peng, *J. Mater. Chem. A*, 2013, **1**, 2144-2150.
37. C.-Y. Chang, Y.-J. Cheng, S.-H. Hung, J.-S. Wu, W.-S. Kao, C.-H. Lee and C.-S. Hsu, *Adv. Mater.*, 2012, **24**, 549-553.
38. M. Ariu, M. Sims, M. D. Rahn, J. Hill, A. M. Fox, D. G. Lidzey, M. Oda, J. Cabanillas-Gonzalez and D. D. C. Bradley, *Phys. Rev. B*, 2003, **67**, 195333.
39. J. Peet, J. Y. Kim, N. E. Coates, W. L. Ma, D. Moses, A. J. Heeger and G. C. Bazan, *Nat. Mater.*, 2007, **6**, 497-500.
40. Z. He, C. Zhang, X. Xu, L. Zhang, L. Huang, J. Chen, H. Wu and Y. Cao, *Adv. Mater.*, 2011, **23**, 3086-3089.
41. L. Li, Y. Huang, J. Peng, Y. Cao and X. Peng, *Org. Electron.*, 2013, **14**, 3430-3436.
42. J. K. Lee, W. L. Ma, C. J. Brabec, J. Yuen, J. S. Moon, J. Y. Kim, K. Lee, G. C. Bazan and A. J. Heeger, *J. Am. Chem. Soc.*, 2008, **130**, 3619-3623.
43. Y. Matsuo, Y. Sato, T. Niinomi, I. Soga, H. Tanaka and E. Nakamura, *J. Am. Chem. Soc.*, 2009, **131**, 16048-16050.
44. W. Chen, M. P. Nikiforov and S. B. Darling, *Energy Environ. Sci.*, 2012, **5**, 8045-8074.
45. M.-S. Su, C.-Y. Kuo, M.-C. Yuan, U. S. Jeng, C.-J. Su and K.-H. Wei, *Adv. Mater.*, 2011, **23**, 3315-3319.
46. C. H. Woo, P. M. Beaujuge, T. W. Holcombe, O. P. Lee and J. M. J. Frechet, *J. Am. Chem. Soc.*, 2010, **132**, 15547-15549.
47. V. Shrotriya, Y. Yao, G. Li and Y. Yang, *Appl. Phys. Lett.*, 2006, **89**, 063505.
48. P. W. M. Blom, M. J. M. deJong and M. G. vanMunster, *Phys. Rev. B*, 1997, **55**, R656-R659.

# Solution-processed bulk heterojunction solar cells based on a porphyrin small molecule with 7% power conversion efficiency

Hongmei Qin,<sup>†</sup> Lisheng Li,<sup>†</sup> Fangqing Guo, Shijian Su, Junbiao Peng, Yong Cao, Xiaobin Peng\*

## Table of contents entry

The solution-processed BHJ solar cells based on a porphyrin small molecule as the donor material exhibit a PCE up to 7.23%.

